DnaJ (Hsp40 Protein) Binding to Folded Substrate Impacts KplE1 Prophage Excision Efficiency

Tania Puvirajesinghe, Latifa Elantak, Sabrina Lignon, Nathalie Franche, Marianne Ilbert, Mireille Ansaldi

THE JOURNAL OF BIOLOGICAL CHEMISTRY VOL. 287, NO. 17, pp. 14169–14177, April 20, 2012

DnaJ (Hsp40 Protein) Binding to Folded Substrate Impacts KplE1 Prophage Excision Efficiency*[S]

Received for publication, December 7, 2011, and in revised form, February 23, 2012 Published, JBC Papers in Press, February 28, 2012, DOI 10.1074/jbc.M111.331462

Tania M. Puvirajesinghe[‡1], Latifa Elantak[§], Sabrina Lignon[¶], Nathalie Franche[‡], Marianne Ilbert[‖], and Mireille Ansaldi[‡2]

From the [‡]Laboratoire de Chimie Bactérienne, CNRS UMR7283, [§]Laboratoire d'Ingénierie des Systèmes Macromoléculaires CNRS UMR7255, the [¶]Proteomic Facility (MaP Marseille Protéomique IBiSA), and [‖]Bioénergétique et Ingénierie des Protéines CNRS UMR7281, Institut de Microbiologie de la Méditerranée, Aix-Marseille University, 31 Chemin Joseph Aiguier, 13402 Marseille Cedex 20, France

Background: DnaJ positively modulates KplE1 prophage excision and is involved in lysogeny escape.
Results: The recombination directionality factor TorI, from KplE1 prophage, interacts with the DnaJ chaperone, and they protect each other from limited trypsin digestion.
Conclusion: DnaJ stabilizes TorI recombination directionality factor conformation.
Significance: DnaJ cochaperone can bind folded substrates and induces the conformational stabilization of the TorI protein.

Temperate phages mediate gene transfer and can modify the properties of their host organisms through the acquisition of novel genes, a process called lysogeny. The KplE1 prophage is one of the 10 prophage regions in *Escherichia coli* K12 MG1655. KplE1 is defective for lysis but fully competent for site-specific recombination. The TorI recombination directionality factor is strictly required for prophage excision from the host genome. We have previously shown that DnaJ promotes KplE1 excision by increasing the affinity of TorI for its site-specific recombination DNA target. Here, we provide evidence of a direct association between TorI and DnaJ using *in vitro* cross-linking assays and limited proteolysis experiments that show that this interaction allows both proteins to be transiently protected from trypsin digestion. Interestingly, NMR titration experiments showed that binding of DnaJ involves specific regions of the TorI structure. These regions, mainly composed of α-helices, are located on a surface opposite the DNA-binding site. Taken together, we propose that DnaJ, without the aid of DnaK/GrpE, is capable of increasing the efficiency of KplE1 excision by causing a conformational stabilization that allows TorI to adopt a more favorable conformation for binding to its specific DNA target.

Site-specific recombination is used by temperate phages to integrate and excise from their host chromosome (1). As a consequence, temperate phages mediate gene transfer and can modify the properties of their host organisms through the acquisition of novel genes, a process called lysogeny (2, 3). The ancient prophage KplE1 (or CPS-53) is one such example, which contains 16 open reading frames and belongs to one of the 10 prophage regions present in the *Escherichia coli* K12 MG1655 (4, 5). Although fully competent for site-specific recombination, KplE1 is noninfectious and defective for virion formation and host cell lysis (6). Therefore, experimental studies of excisive recombination are made easier by the defective nature of the KplE1 prophage, because the host cells do not lyse upon prophage induction. The KplE1 integrase protein, IntS, belongs to the tyrosine recombinase family of integrases, which are exemplified by the prototypic member phage λ. In addition to the integrase protein, prophage excision from the chromosome requires additional proteins, which are classed as recombination directionality factors (RDFs)[3] (7). TorI is the RDF of KplE1 and is essential for prophage excision (8). It is encoded by the *torI* gene, which is located upstream of the 3′ core sequence that marks the end of the prophage (6). Some RDFs, such as Cox proteins of phages P2 and HP1, have additional regulatory functions outside recombination (9). TorI itself was originally identified as a negative response regulator of the TorR protein, which activates transcription of the *torCAD* operon, encoding the trimethylamine-*N*-oxide reductase respiratory system (10).

Molecular chaperones are widely distributed in all organisms and are involved in protein folding, maturation, and disaggregation (11). Remodeling of protein complexes is also part of the molecular chaperone functions and involves the interaction with native substrates (12). DnaJ (Hsp40) is a cochaperone that regulates the protein folding function of DnaK (Hsp70) chaperone by binding and delivering substrates to DnaK as well as activating ATP hydrolysis (13). DnaJ is universally conserved in biological kingdoms (14). Classical functions of the DnaK/DnaJ/GrpE machinery under low stress conditions include folding of newly synthesized proteins, protein assembly and disassembly, and translocation of proteins into organelles (15,

* This work was supported by CNRS, the French Research Ministry (Ministère de l'Éducation Nationale, de la Recherche et de la Technologie), and National Research Agency Grant ANR-08-BLAN-0122-01.
[S] This article contains supplemental Figs. S1–S3 and Table S1.
[1] Present address: Polarité Cellulaire Signalisation et Cancer, Centre de Recherche en Cancérologie de Marseille, Inserm U1068, CRCM, 27, Bd Lei Roure, 13009 Marseille, France.
[2] To whom correspondence should be addressed: Laboratoire de Chimie Bactérienne CNRS UMR7283, Institut de Microbiologie de la Méditerranée, Aix-Marseille University, 31 Chemin Joseph Aiguier, Marseille 13009, France. Tel.: 33-491164585; Fax: 33-491718914; E-mail: ansaldi@imm.cnrs.fr.

[3] The abbreviations used are: RDF, recombination directionality factor; BMH, bismaleimidohexane; IHF, integration host factor; Tricine, *N*-[2-hydroxy-1,1-bis(hydroxymethyl)ethyl]glycine.

16). Under conditions of cellular stress, DnaJ, together with DnaK and GrpE, play a role in the protection of proteins against stress-induced unfolding as well as refolding of unfolded proteins (17). The initial discovery of DnaJ is exquisitely intertwined with initial research into phage λ DNA replication (18). DnaJ was found to be involved in recruiting DnaK into the preinitiation complex at the phage origin of replication (19). In this process, DnaJ binds first to the replication initiation protein λP and the host primase DnaB in the preprimosomal complex. This allows recruitment of DnaK and subsequent binding to λP, which in turn results in the release of the preinitiation complex thus initiating DNA replication (19, 20). Besides its cochaperone function, DnaJ is involved in several functions. DnaJ from *E. coli* possesses an active dithiol/disulfide group, which has been suggested to allow DnaJ to control the redox state of cytoplasmic, membrane, or exported proteins (21). DnaJ is also known to act as a holdase chaperone that does not actively refold protein clients but can bind hydrophobic exposed surfaces of unfolded substrates and prevent their aggregation (22). Additionally, DnaJ-like proteins have been implicated in viral infection of plants. A DnaJ-like protein has been identified from *Nicotiana tabacum,* designated MP-interacting protein 1 (NtMPIP1), which has been shown to interact with the essential movement protein of tobacco mosaic virus, thereby implicating DnaJ as a host-encoded factor involved in the cell-to-cell spread of tobacco mosaic virus (23).

As mentioned above, in *E. coli* the DnaK/DnaJ/GrpE machinery has been discovered through its role in λ phage replication. Recently, we have shown that DnaJ is also involved in prophage excision of a class of (pro)phages that share very similar recombination modules (24). As this role appeared to be a *bona fide* chaperone activity of DnaJ, which was independent of DnaK, we have now further characterized the structural features underlying the TorI/DnaJ interaction.

EXPERIMENTAL PROCEDURES

Overproduction and Purification of TorI—TorI was produced from *E. coli* BL21 (DE3) harboring plasmid pETsI, as described previously (6).

Overproduction and Purification of DnaJ—DnaJ was produced using pGPJ-His (25) in the Δ^5 strain (MC4100 *dnaK-dnaJ42*::*kan, grpE*::*tet cbpA*::*kan, djlA*::*spc*, laboratory strain from P. Genevaux). Fresh overnight cultures were diluted 1:100 in 500 ml of LB broth supplemented with 100 $\mu g/ml^{-1}$ ampicillin and grown with vigorous shaking at 30 °C. Cultures were induced with L-arabinose 0.2% (w/v) and incubated for a further 4 h. Cells were harvested and resuspended in 30 ml of buffer 1 (40 mM sodium phosphate buffer, pH 7.4, 20 mM imidazole, 0.6% Brij 58P, 0.5% Triton, 1 M NaCl, 20 mM β-mercaptoethanol). Cells were lysed using a French press, and lysates were centrifuged at 40,000 rpm for 1 h in a Beckman 70 Ti rotor. The supernatant was isolated and filtered using a 0.2-μm filter. The sample was loaded onto a nickel Hi-Trap FF 1-ml column (GE Healthcare). The column was washed with buffer 2 (50 mM sodium phosphate, 20 mM imidazole, 1 M NaCl, 20 mM β-mercaptoethanol). Proteins were then eluted using buffer 2 containing 250 mM imidazole. The protein buffer was then exchanged into storage buffer (40 mM sodium phosphate, pH 7.6, 100 mM KCl, 10% glycerol, 1 mM DTT), and the protein was stored at −80 °C.

Immunoblot Analysis—Proteins were prepared using 2× SDS-Tricine sample buffer and heated to 95 °C for 10 min. Samples were separated according to their molecular weight by SDS-Tricine gel electrophoresis and transferred to nitrocellulose membranes for immunoblotting. Membranes were blocked at 25 °C for 1 h with phosphate-buffered saline (PBS) containing 5% skimmed milk powder. Blots were incubated overnight with a primary antibody, either rabbit polyclonal primary antibodies recognizing DnaJ (diluted 1:1,000) or rabbit polyclonal primary antibodies recognizing TorI (diluted 1:10,000). Blots were washed three times with PBS. Anti-rabbit HRP-conjugated antibody (1:10,000, Amersham Biosciences) was used as a secondary antibody and incubated for 1 h at room temperature. After washing three times with PBS, blots were developed with ECL Supersignal West Pico chemiluminescent substrate (Thermo Scientific).

In Vitro Chemical Cross-linking—Cross-linking experiments were carried out using bismaleimidohexane (BMH) cross-linking reagent (Pierce). Proteins (2–4 μg) were incubated for 30 min at room temperature in PBS buffer containing 300 mM KCl and 1 mM BMH. Samples were analyzed using 12% SDS-Tricine gels followed by PageBlue (Fermentas) protein stain and immunoblotting analysis.

Far-UV Circular Dichroism—Far-UV CD spectra were recorded on a Jasco 815 CD spectrometer using 2-mm thick quartz cells (10 mm path length) in 40 mM sodium phosphate, pH 7.4, and 100 mM KCl at 20 °C. CD spectra were measured from 190 to 260 nm, with a scanning speed of 10 nm/min, and results were averaged from five scans. All spectra were buffer-corrected and normalized for any variation in protein concentrations. Protein concentrations used were as follows: TorI, 25 μM; DnaJ, 0.8 μM or 0.25 μM.

Limited Trypsin Digestion and Mass Spectrometry Analysis—DnaJ and TorI proteins were incubated alone and together, in the presence of trypsin, which was used at a 1:100 (trypsin/total protein, w/w). Enzymatic digestion was started by addition of trypsin, and the reaction was carried out at room temperature. Aliquots were taken at different time points of the enzyme digestion. Samples were spotted with a saturated solution of sinapinic acid matrix (40% acetonitrile in water, 0.1% trifluoroacetic acid (v/v)) directly onto a MALDI plate. Mass spectrometric analysis was carried out using a Microflex MALDI-TOF mass spectrometer (Bruker Daltonics). Mass determination was performed in positive linear mode to analyze monomeric proteins forms and in positive reflectron mode for tryptic peptides. Peptide mass fingerprint analysis was processed by Biotools software using internal calibration (26).

Alternatively, trypsin digestion of samples was stopped by heating samples to 99 °C for 5 min and analyzed on a 12% SDS-Tricine gel or by using an automated Experion separation system (supplemental Fig. S2). Samples were loaded onto a Pro260 chip run following the manufacturer's instructions. Data analysis used Experion Software (version 3.0).

NMR Titration Experiments—TorI was labeled by growing cells in M9 minimal medium supplemented with 1 g/liter $[^{15}N]NH_4Cl$ (Cambridge Isotopes), supplemented with ampi-

cillin (100 μg/ml), thiamine (2 pg/ml), $MgSO_4$ (1 mM), $CaCl_2$ (0.1 mM). TorI protein was purified as described previously (16). Titration experiments were carried out in 20 mM HEPES, pH 7.2, 50 mM KCl, 5% glycerol, 10% D_2O as follows: 0.05, 0.1, and 0.2 mM final concentration of ^{15}N-labeled TorI (0.5, 1, and 2 molecular equivalents) were added to 0.1 mM unlabeled DnaJ. Chemical shift perturbations in TorI were monitored in two-dimensional ^{1}H-^{15}N HSQC experiments. Weighted average chemical shift variations were calculated according to the formula, $\Delta ppm = ((\Delta\delta_{HN})^2 + (\Delta\delta_N \times 0.17)^2)1/2$ (27). The NMR experiments have been recorded at 290 K on a 600 MHz spectrometer (Avance III 600 MHz Bruker) equipped with a cryoprobe.

Site-specific Mutagenesis of TorI α3 Helix—To construct plasmid pETsI-R63C-A64S, the codons corresponding to residues Arg^{63} and Ala^{64} were replaced by Cys and Ser codons, respectively, by a one-step PCR method (28) using plasmid pETsI as a template and overlapping divergent primers Ir-61–63-64 (5′-CTTATTTTTGAATTCACAATGGTCACGATATAACC) and Im-R63C-A64S (5′-TGTGAATTCAAAAATAAGCTCTTAAGCTGCTCCAATGGGTAACTC). The sequence accuracy of the construction was checked by direct sequencing. The mutant protein (TorI_R63C_A64S) was produced in a C41 *E. coli* strain and purified as the wild type.

In Vitro Excision Assay—Linear *att* sites were amplified by PCR with primer pairs attLSpeI/attL-KpnI for *att*L and attR-XbaI/attR-IHF2 for *att*R and then purified using QIAQuick PCR purification kit protocol (Qiagen). Reaction mixtures (50 μl) included linear *att* DNA sites (28 nM) in buffer containing 33 mM Tris-HCl, pH 7.6, 33 mM KCl, 9 mM spermidine, 4 mM EDTA, 0.9 mg/ml^{-1} BSA, and 7% glycerol, IHF (0.3 μM), and IntS (0.6 μM). TorI and DnaJ were added at the same molarity: TorI WT (0.7 μM), DnaJ (0.7 μM), or TorI*63–64 (2.1 μM), DnaJ (2.1 μM). TorI and DnaJ were initially preincubated at 37 °C for 30 min, and then IntS, IHF, and linear *att*L and *att*R DNA were simultaneously added. The reactions were carried out in optimized conditions at 30 °C for 2 h at an IHF/IntS/TorI/DnaJ protein ratio of 1:2:2.3:2.3 for TorI WT and 1:2:7:7 for TorI_R63C_A64S. Reaction products were purified (QIAQuick kit, Qiagen) and analyzed on a 2% agarose gel electrophoresis.

RESULTS AND DISCUSSION

Direct Association of DnaJ and TorI—We have previously shown that DnaJ has the ability to increase the excision efficiency of the KplE1 prophage from the K12 bacterial chromosome (24). The presence of DnaJ increased the affinity of TorI for its specific DNA targets on *att*L. However, we also showed that DnaJ was released from the *att*L-TorI complex, suggesting a dynamic complex and a *bona fide* chaperone role for DnaJ. To fully understand this functional role of DnaJ, it was crucial to characterize the protein/protein interaction with the TorI RDF. The *in vitro* behavior of purified protein preparations of $DnaJ_{His6}$ and TorI proteins in the presence of BMH, a cysteine-reactive cross-linker with an 8-Å spacer arm, was initially analyzed. Proteins were incubated individually or together in the presence of BMH and separated using 12% Tricine-SDS gels. Proteins were then transferred onto nitrocellulose membrane and analyzed by immunoblotting for TorI or DnaJ (Fig. 1). In the presence of BMH, immunoblot analysis showed a characteristic oligomerization of TorI when incubated alone (29). This was seen by the presence of bands corresponding to dimeric through to hexameric forms of TorI (Fig. 1, *left panel*). When DnaJ was incubated with BMH cross-linker, DnaJ was mainly present as monomers (Fig. 1, *right panel*). When TorI and DnaJ were incubated together, in the presence of BMH, an extra band of ~50 kDa was revealed with TorI and DnaJ antisera. The proportion of this DnaJ-TorI complex consequently increased when TorI was incubated with a higher concentration of DnaJ. The apparent size of the TorI-DnaJ complex was compatible with a 1:1 DnaJ/TorI ratio (DnaJ, 41.9 kDa and TorI, 7.7 kDa).

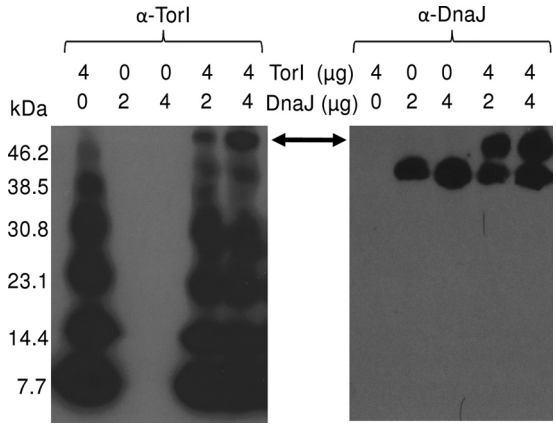

FIGURE 1. **Direct association of DnaJ with TorI.** *In vitro* chemical cross-linking of DnaJ and TorI shows a direct association between DnaJ and TorI. Purified proteins were cross-linked with BMH (Pierce). Increasing concentrations of DnaJ (2 and 4 μg) were incubated with TorI protein (4 μg). Proteins were separated using 12% Tricine-SDS gels, blotted, and immunodetected with TorI or DnaJ antisera. A *double-sided arrow* points to the protein bands containing the TorI-DnaJ complex in both blots.

DnaJ Induces a Structural Change in TorI—The far-UV CD spectrum of TorI (200–250 nm) displayed a double-peaked band with minima at 208 and around 220 nm characteristic of the presence of α-helices in the three-dimensional structure (Fig. 2, *black line*), which was consistent with the solution structure of TorI (8). To analyze whether structural changes occurred upon interaction of TorI with DnaJ, we monitored the effect of DnaJ on the structural conformation of TorI by adding low quantities of DnaJ (TorI/DnaJ ratio 25:0.8 or 25:0.2). Such amounts of DnaJ should allow the observation of an effect of DnaJ on the secondary structure of TorI without perturbing the spectrum. Indeed, under these conditions the CD spectrum of DnaJ by itself is identical to that of the buffer (data not shown). Interestingly, in the presence of DnaJ, the TorI CD spectrum shifted downwards, indicating that TorI undergoes conformational changes with an overall gain in helical structure, and this effect varied with the DnaJ concentration used (Fig. 2, *light* and *dark gray lines*). When the same experiment was carried out with lysozyme, instead of DnaJ, using similar concentrations, there was no change in the CD signal of TorI (supplemental Fig. S1). This therefore suggested that a discrete, but significant, structural change on the TorI RDF is specifically due to the presence of DnaJ. Noticeably, substoichiometric amounts of DnaJ were used, and we would expect a more drastic change to occur with higher concentrations of DnaJ; however, in this case the contribution of DnaJ to the CD spectrum would not be

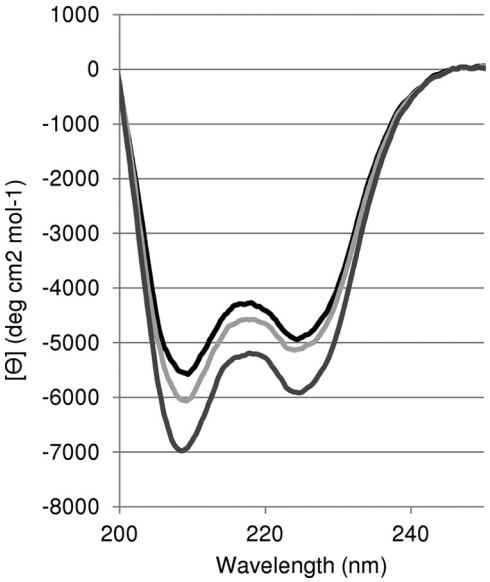

FIGURE 2. **Change in ellipticity of the TorI protein upon incubation with DnaJ.** TorI ellipticity was measured using a Jasco 815 CD spectrometer. *Black curve* is relevant to the spectrum obtained with TorI alone, and the *gray curves* were obtained in the presence of DnaJ (*light gray*, 0.25 μM; *dark gray*, 0.8 μM).

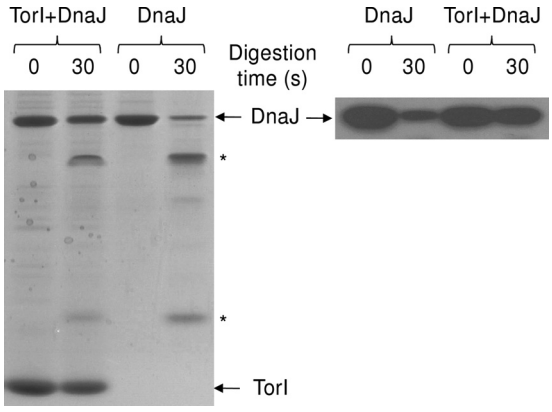

FIGURE 3. **DnaJ is transiently protected from trypsin digestion in the presence of TorI.** TorI (8 μg) and DnaJ (2 μg) proteins were mixed with trypsin (1:100 trypsin/protein ratio) and incubated at 37 °C for 30 s. Digestion products were separated using a 16% Tricine-SDS-PAGE. The digestion profile of DnaJ was analyzed by immunoblot with polyclonal rabbit anti-DnaJ antibody. *Arrows* point to full-length DnaJ and TorI, and *asterisks* label digestion fragments of DnaJ.

neutral. Overall, this preliminary experiment strongly suggests that the DnaJ interaction with TorI slightly modifies the TorI conformation thus allowing more efficient binding to DNA.

DnaJ Is Protected from Trypsin Digestion When Incubated with TorI—The behavior of the DnaJ and TorI complex was further studied by limited proteolysis in the presence of the serine protease trypsin. The effect of trypsin digestion on DnaJ was initially analyzed after 30 s of enzyme digestion, by Tricine-SDS-polyacrylamide gel separation. Prior to trypsin digestion, the monomeric form of DnaJ was detected as a single gel band at 42 kDa under reducing conditions (Fig. 3, *left panel*). When trypsin was added using a 1:100 trypsin/protein ratio, a reduction of the full-length form of DnaJ was observed, and resulting digestion fragment peptides were produced that were not present in the undigested DnaJ sample. In the presence of TorI, an additional band appeared at 7.7 kDa, which corresponds to the full-length form of TorI. However, when DnaJ was digested by trypsin, using the same trypsin/protein ratio, a higher amount of DnaJ remained after 30 s of trypsin digestion than was seen when DnaJ was digested alone. This was further confirmed by transferring the proteins onto nitrocellulose membrane and immunoblotting using a DnaJ-specific antibody (Fig. 3, *right panel*). DnaJ interacts directly with TorI (Fig. 1), and this interaction confers a protection to trypsin to DnaJ either by direct protection of trypsin sites or by an induced conformational change. The level of protection of DnaJ by TorI upon trypsin digestion was quantitatively estimated by automated SDS-PAGE separation (Experion). Amounts of full-length DnaJ protein before and after trypsin digestion were measured, in the presence and absence of TorI (supplemental Fig. S2). The analysis suggested that 46% of the initial amount of DnaJ remained after 30 s of trypsin digestion, when DnaJ was digested alone. However, when TorI was present, 60% of the initial amount of DnaJ remained after 30 s of trypsin digestion. These results suggested that DnaJ was protected from trypsin digestion upon incubation with TorI.

TorI Is Transiently Protected from Limited Proteolysis in the Presence of DnaJ—Limited proteolysis digestion by trypsin was performed under the same conditions as before and was achieved by taking aliquots at progressive time points of the digestion (0, 3, 30, 90, and 120 s). It should be noted that the level of protection of TorI by DnaJ upon trypsin digestion was unable to be estimated due to the limiting resolution of small proteins with the Experion protein chip. Samples were thus initially analyzed using linear mode mass determination MALDI-TOF mass spectrometry because the TorI protein is too small to analyze using denaturing gel electrophoresis (Fig. 4*A*, *left panel*). The undigested form of TorI appeared at (7,680 ± 1.5 Da). Data showed that when alone, TorI was digested very quickly with trypsin because after 90 s of digestion the full-length TorI could no longer be detected. Trypsin-generated TorI fragments were present shortly after trypsin addition as seen at 3 s. However, in the presence of DnaJ, trypsin-generated TorI fragments did not appear as rapidly (Fig. 4*A*, *right panel*). Indeed, after 90 s of digestion, the global mass of undigested TorI could still be detected. However, at 120 s, full-length TorI had totally disappeared in both the presence and absence of DnaJ. This suggested that the presence of DnaJ was able to transiently protect TorI from digestion with trypsin.

Detailed analysis of the digestion peptides resulting from limited proteolysis of TorI, was then undertaken using reflectron mode MALDI-TOF mass spectrometry, and the data were summarized in Fig. 4*B*, Table 1, and supplemental Table S1. Peptides were numbered, and their presence was noted for each time point (0, 3, 90, and 120 s) in each condition, when TorI protein was alone and when TorI and DnaJ were together (Table 1 and supplemental Table S1). Trypsin cleaves at the C terminus of lysine or arginine residues in an amino acid sequence, and 12 trypsin cleavage sites are predicted in the TorI amino acid sequence. Trypsin digestion of TorI produced a good sequence coverage (at least 89.4% sequence coverage MS) with 30 peptides identified out of 69 theoretical trypsin peptides (as computed with BioTools with up to six miscleavages allowed). The digestion pattern of TorI was substantially differ-

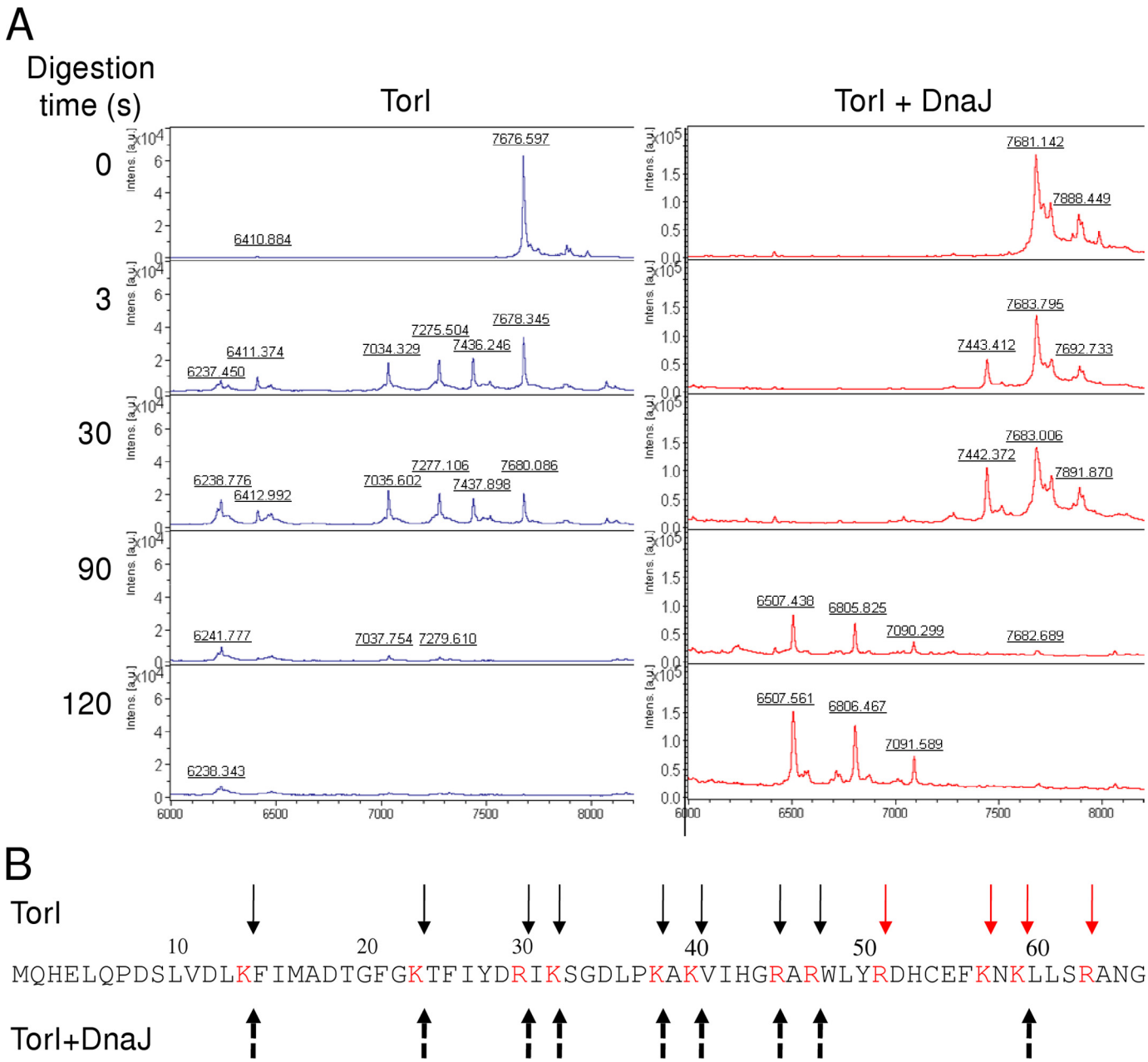

FIGURE 4. **Monomeric TorI is protected from trypsin digestion in the presence of DnaJ.** Limited proteolysis with trypsin was carried out for the TorI and DnaJ proteins together and alone. Samples were analyzed using MALDI-TOF MS using two different modes of peptide determination. *A,* linear mode MALDI-TOF MS analysis showed monomeric TorI remained in excess in the digestion fragment peaks until 90 s. However, in the absence of DnaJ, TorI was more quickly digested, with the digestion fragment peaks appearing after only 3 s of trypsin digestion. *B,* cleavage sites of trypsin in TorI are indicated by *arrows*, and missing cleavage sites in the presence of DnaJ are indicated in *red* (amino acids 51, 57, 59, and 63). These amino acids mapped onto the C-terminal α-helix of the TorI structure.

ent in the presence of DnaJ. Certain regions of TorI were transiently protected from trypsin digestion in the presence of DnaJ, and cleavage in these regions only appeared at later time points of digestion. After 3 s of trypsin digestion, peptides appearing from cleavage at amino acids 51, 57, 59, and 63 only appeared when TorI was alone and not when DnaJ was present with TorI.

Together, limited trypsin digestion experiments indicated a transient protection of TorI and DnaJ on each other, which confirmed the formation of a transient complex of the two proteins, and this complex involves the C-terminal region of TorI either directly or indirectly through discrete conformational changes of this region.

Mapping of Amino Acid Residues Implicated in the Formation of TorI-DnaJ Complex by Heteronuclear NMR—An NMR titration experiment was carried out to locate the amino acid residues at the surface of the TorI structure, which were involved in binding to DnaJ. This was achieved by titrating isotopically labeled ^{15}N-TorI with unlabeled DnaJ, and the reaction was carried out at 25 °C. Chemical shift variations were monitored using two-dimensional ^{1}H-^{15}N HSQC spectra (supplemental Fig. S3). Significant chemical shift perturbations

TABLE 1

TorI peptides detected upon trypsin hydrolysis in the presence or absence of DnaJ

Transient protection of specific trypsin cleavage sites in the TorI amino acid sequence was analyzed. TorI cleavage peptides were identified using reflectron mode MALDI-TOF MS analysis and listed at each time point of trypsin digestion (0, 3, 30, 90 and 120 s). 1 indicates the presence of a given peptide in the sample; 0 indicates its absence.

Numerical assignment[a]	Peptide size (amino acid)	Digestion time 3 s		Digestion time 30 s		Digestion time 90 s		Digestion time 120 s	
		TorI	DnaJ + TorI	TorI	DnaJ + TorI	TorI	DnaJ + TorI	TorI	DnaJ + TorI
1	66	1	1	1	1	0	0	0	0
2	45	1	1	1	1	0	0	0	0
3	40	1	1	1	1	0	0	0	0
4	38	1	1	1	1	0	0	0	0
5	32	1	1	1	1	1	1	1	1
6	30	1	1	1	1	1	1	1	1
7	24	1	1	1	0	1	1	1	1
8	14	1	0	1	0	1	1	1	1
9	31	1	1	1	1	1	1	0	0
10	26	1	1	1	0	0	0	0	0
11	24	0	0	1	1	0	0	0	0
12	18	1	1	1	1	1	1	1	0
13	16	1	1	1	1	1	1	1	1
14	10	1	0	1	0	1	1	1	1
15	21	1	0	0	0	0	0	0	0
16	18	1	0	1	0	0	0	0	0
17	14	1	1	1	1	1	1	1	0
18	12	1	0	1	0	1	1	1	0
19	19	1	1	0	0	0	0	0	0
20	16	1	0	0	0	0	0	0	0
21	12	1	0	1	1	1	1	1	1
22	10	1	0	1	0	1	1	1	1
23	31	0	0	1	0	0	0	0	0
24	15	0	0	1	0	0	0	0	0
25	27	0	0	0	0	0	0	1	0
26	8	0	0	0	0	1	0	0	0
27	6	1	0	1	0	1	1	1	1
28	8	1	0	1	0	1	1	1	1
29	6	0	0	0	0	0	0	1	0
30	8	0	0	0	0	0	0	1	0
31	6	0	0	1	1	0	0	0	0
Total		23	13	24	13	15	14	16	12

[a] Numerical assignment refers to supplemental Table S1.

were observed upon the addition of increasing amounts of ^{15}N-labeled TorI to unlabeled DnaJ, indicative of equilibrium between the bound and unbound states in the fast exchange regime. The weighted average chemical shift displacements are shown in Fig. 5*A*. The largest chemical shift variations between the free and the bound forms of TorI are mainly observed for backbone amides of the first β-strand (Gln^{6}, Ser^{9}, Leu^{10}, and Val^{11}), the helix α1 (Ile^{16}, Asp^{19}, and Gly^{21}), the β3-strand involved in anti-parallel β-sheet flexible loop region (Arg^{47}), and the C-terminal helix 3 (Glu^{55}, Lys^{57}, Lys^{59}, Leu^{61}, Arg^{63}, and Ala^{64}). These latter perturbations are in agreement with the mass spectrometry data showing the protection of the TorI C-terminal part in the presence of DnaJ. The perturbed residues congregate onto one face of the TorI protein surface opposite the TorI DNA-binding site, which we have previously mapped (Fig. 5, *B* and *C*) (8). Indeed, none of the residues involved in the interaction with DNA were perturbed upon DnaJ binding. However, some residues (Leu^{10}, Val^{11}, and Ile^{16}) are very close to the wing and the helix α1 contacting DNA. This close proximity of the DnaJ and DNA-binding sites on TorI structure may have a direct influence on the observed increased affinity of TorI for DNA (24).

To validate whether the residues identified by NMR were involved in a direct interaction with DnaJ, we constructed three different TorI mutants, TorI_L10Q_V11S, TorI_L61S, and TorI_R63C_A64S, that behaved differently in terms of their protein production and stability. TorI_L10Q_V11S proved to be very unstable and was barely produced. TorI_L61S was produced and stable, but this single substitution was insufficient to disrupt the TorI/DnaJ interaction (data not shown). Finally, the double mutant TorI_R63C_A64S was stably produced and showed the same overall structure as the wild-type protein by CD (data not shown). This latter mutant was affected in DnaJ binding as shown in Fig. 6*A*, thus validating that the residues identified and mapped through NMR titration assay were indeed involved in DnaJ binding. This double-substituted protein was assayed *in vitro* for its propensity to recruit DnaJ in a recombination assay. As seen in Fig. 6*B*, the TorI_R63C_A64S, although active in an *in vitro* excision assay, failed to recruit DnaJ. As a result, no increased efficiency in the presence of DnaJ was observed in contrast to what was observed when the wild-type protein was used. Together, these results confirm the results obtained by NMR titration indicating that the C-terminal α-helix in TorI was important for DnaJ recruitment.

Conclusions—We have previously identified a functional role of DnaJ in assisting prophage excision (24). Initial experimental data showed that DnaJ did not bind to the *att*L DNA itself but somehow increased the affinity of TorI for this site. Here, we have shown that DnaJ binds directly to the TorI RDF inducing a stabilization of its conformation. Taken together, the data shown here demonstrate that DnaJ interacts with a folded substrate, TorI. This interaction results in a transient and reciprocal protection of these two proteins, either due to direct binding or to induced conformational change. Conclusions drawn from

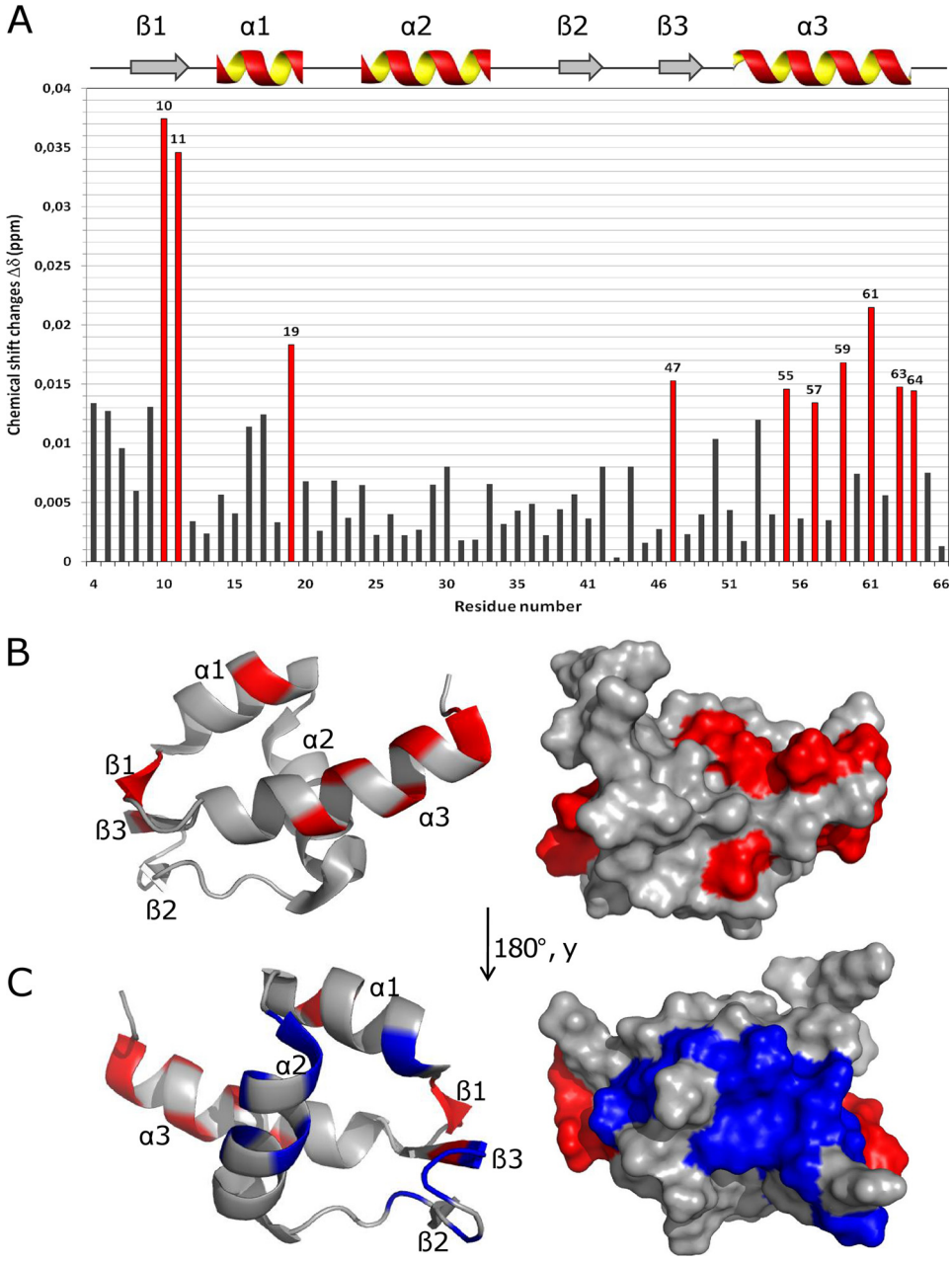

FIGURE 5. **Mapping the binding site of DnaJ in the TorI structure by heteronuclear NMR.** *A*, plot of the weighted average chemical shift variations of ^{15}N-TorI backbone upon binding of DnaJ. Secondary structures of TorI are shown *above* the plot. The *red bars* correspond to residues showing the largest chemical shift variations. *B*, chemical shift mapping onto *ribbon* (*right*) and surface (*left*) representations of TorI. Residues undergoing the largest chemical shift changes upon DnaJ binding are colored in *red*. *C*, ribbon (*right*) and surface (*left*) representations of the data presented in *B*, after 180° rotation according to the *y* axis, with the residues involved in DNA binding colored *blue*.

both NMR and CD experiments led us to propose that DnaJ has an atypical effect on a native protein that induces conformational α-helix stabilizations. The NMR data collected provides information on the residues that are or are not trypsin cleavage sites. If we look at residues that undergo a chemical shift and that are also transiently protected from trypsin, we can identify residues Arg^{47}, Lys^{57}, Lys^{59}, and Arg^{63}, many of which lie in the C-terminal helix of TorI.

The ^{1}H-^{15}N HSQC spectrum of TorI upon binding of DnaJ does not show dramatic modifications that could correspond to important conformational changes of the protein. However, CD experiments suggest that slight structural modifications occur in TorI when in the presence of DnaJ (Fig. 2). The residues perturbed upon binding of DnaJ on TorI in the NMR experiments are mostly located within α-helices of TorI. Binding of DnaJ might then have the effect of stabilizing the helices as illustrated by the downward shift in the CD signal of TorI. This could provide a stabilizing effect, which probably helps to position TorI to obtain optimal binding to its target DNA.

How and when TorI is released from DnaJ still remains unknown. We show that the segment of TorI that interacts with *att*L is not altered upon binding to the DnaJ protein. This means that there are two possible models, either DnaJ acts at the same time as TorI with *att*L or prepares TorI beforehand for

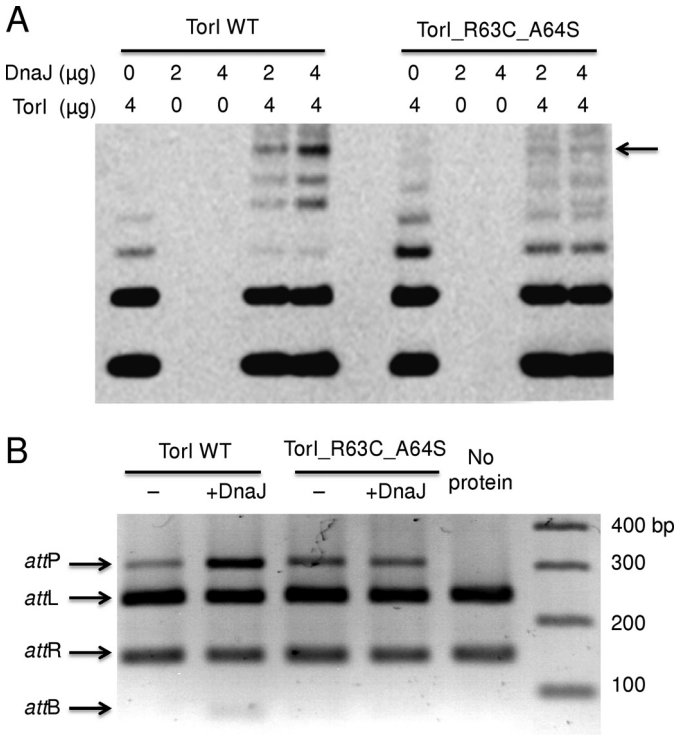

FIGURE 6. **Critical residues for DnaJ interaction in TorI C-terminal α-helix.** *A, in vitro* chemical cross-linking of DnaJ and TorI (TorI WT or TorI_R63C_A64S) under the same conditions defined as in Fig. 1. Proteins were separated using 12% Tricine-SDS gels, blotted, and immunodetected with TorI antiserum. An *arrow* points the TorI-DnaJ complex. *B, in vitro* excision assay in the presence of DnaJ and TorI (TorI WT or TorI_R63C_A64S). *In vitro* excision assays were performed with suboptimal concentrations of recombination proteins (0.6 μM IntS, 0.3 μM IHF, and 0.7 μM TorI WT or 2.1 μM TorI_R63C_A64S). DnaJ was added at the same concentration as TorI WT or mutant when indicated (0.7 and 2.1 μM DnaJ, respectively).

binding to *att*L. From previous work, we provide evidence to support the latter model, as DnaJ is released and not part of the complex when TorI binds to its specific DNA target *att*L (24), thereby supporting the latter model of a transient interaction of TorI/DnaJ, which prepares TorI to bind DNA. It is still possible that another conformational change may arise on TorI upon binding to DNA, which could be important in the release DnaJ.

Residues experiencing a chemical change in their environment when TorI was incubated with DnaJ do not match the consensus binding motif found in proteins bound by DnaJ (22). Indeed, none of the residues we identified are aromatic, and few are hydrophobic. However, chemical shift perturbation mapping focuses on backbone amide groups only, and one cannot exclude the involvement of the neighboring aromatic and/or aliphatic side chains in the interaction process. Moreover, the amino acid residues that underwent a change in chemical shift upon DnaJ interaction are discontinuous on the primary sequence. This work thus unveils an atypical binding site for DnaJ on a folded substrate. However, at this stage, we cannot fully distinguish if the two perturbed regions are equally involved in DnaJ binding, suggesting a real discontinuous binding site or if binding to one region induces a perturbation on the other region as described for the interaction of DnaK and DnaJ with σ^{32} (30). The C-terminal helix of TorI is highly contacted by DnaJ, with 6 of the 13 interacting residues lying in this helix. Several mutations were performed in this region, and a double substitution R63C/A64S reduced the binding of TorI to DnaJ, clearly demonstrating that the C-terminal helix is directly involved in DnaJ recruitment (Fig. 6). It is important to note that this C-terminal helix of TorI is the only part of the tertiary protein structure that is different from the prototypic excisionase protein from bacteriophage λ (16). TorI and other related RDFs may have evolved extra structural units that recruit accessory factors like DnaJ to regulate excisive recombination. Such RDFs are also found in HK620 and Sf6 phages, as their recombination module, including the integrase and RDF genes, are highly homologous (6). However, a survey of RDF three-dimensional structures would be necessary to identify potential RDF clients of the DnaJ cochaperone.

Acknowledgments—We thank R. Lebrun from the IMM Proteomic Platform (CNRS, Marseille, France) for advice and informative discussions on mass spectrometry analysis. We also thank Y. Denis for help with the use of the Experion apparatus at the IMM Transcriptomic facility (CNRS, Marseille). We are extremely grateful to S. Champ, R. Menouni, G. Panis, and P. Genevaux for stimulating discussions. We thank an anonymous referee for helpful suggestions.

REFERENCES

1. Nash, H. (1996) in *Escherichia coli and Salmonella: Cellular and Molecular Biology* (Neidhardt, F. C., Curtiss, III, R., Ingraham, J. L., Lin, E. C. C., Low, K. B., Magasanik, B., Reznikoff, W. S., Riley, M., Schaechter, M., and Umbarger, H. E., eds) pp. 2363–2376, American Society for Microbiology, Washington, D. C.
2. Canchaya, C., Fournous, G., Chibani-Chennoufi, S., Dillmann, M. L., and Brüssow, H. (2003) Phage as agents of lateral gene transfer. *Curr. Opin. Microbiol.* **6,** 417–424
3. Brüssow, H., Canchaya, C., and Hardt, W. D. (2004) Phages and the evolution of bacterial pathogens. From genomic rearrangements to lysogenic conversion. *Microbiol. Mol. Biol. Rev.* **68,** 560–602
4. Rudd, K. E. (1999) Novel intergenic repeats of *Escherichia* coli K-12. *Res. Microbiol.* **150,** 653–664
5. Casjens, S. (2003) Prophages and bacterial genomics. What have we learned so far? *Mol. Microbiol.* **49,** 277–300
6. Panis, G., Méjean, V., and Ansaldi, M. (2007) Control and regulation of KplE1 prophage site-specific recombination. A new recombination module analyzed. *J. Biol. Chem.* **282,** 21798–21809
7. Lewis, J. A., and Hatfull, G. F. (2001) Control of directionality in integrase-mediated recombination: examination of recombination directionality factors (RDFs). Including Xis and Cox proteins. *Nucleic Acids Res.* **29,** 2205–2216
8. Elantak, L., Ansaldi, M., Guerlesquin, F., Méjean, V., and Morelli, X. (2005) Structural and genetic analyses reveal a key role in prophage excision for the TorI response regulator inhibitor. *J. Biol. Chem.* **280,** 36802–36808
9. Esposito, D., Wilson, J. C., and Scocca, J. J. (1997) Reciprocal regulation of the early promoter region of bacteriophage HP1 by the Cox and Cl proteins. *Virology* **234,** 267–276
10. Ansaldi, M., Théraulaz, L., and Méjean, V. (2004) TorI, a response regulator inhibitor of phage origin in *Escherichia coli*. *Proc. Natl. Acad. Sci. U.S.A.* **101,** 9423–9428
11. Bukau, B., Weissman, J., and Horwich, A. (2006) Molecular chaperones and protein quality control. *Cell* **125,** 443–451
12. Hartl, F. U., and Hayer-Hartl, M. (2009) Converging concepts of protein folding in vitro and in vivo. *Nat. Struct. Mol. Biol.* **16,** 574–581
13. Szabo, A., Langer, T., Schröder, H., Flanagan, J., Bukau, B., and Hartl, F. U. (1994) The ATP hydrolysis-dependent reaction cycle of the *Escherichia coli* Hsp70 system DnaK, DnaJ, and GrpE. *Proc. Natl. Acad. Sci. U.S.A.* **91,** 10345–10349
14. Kampinga, H. H., and Craig, E. A. (2010) The HSP70 chaperone machin-

ery. J proteins as drivers of functional specificity. *Nat. Rev. Mol. Cell Biol.* **11,** 579–592
15. Genevaux, P., Georgopoulos, C., and Kelley, W. L. (2007) The Hsp70 chaperone machines of *Escherichia coli*. A paradigm for the repartition of chaperone functions. *Mol. Microbiol.* **66,** 840–857
16. Genevaux, P., Keppel, F., Schwager, F., Langendijk-Genevaux, P. S., Hartl, F. U., and Georgopoulos, C. (2004) *In vivo* analysis of the overlapping functions of DnaK and trigger factor. *EMBO Rep.* **5,** 195–200
17. Langer, T., Lu, C., Echols, H., Flanagan, J., Hayer, M. K., and Hartl, F. U. (1992) Successive action of DnaK, DnaJ, and GroEL along the pathway of chaperone-mediated protein folding. *Nature* **356,** 683–689
18. Georgopoulos, C. (2006) Toothpicks, serendipity, and the emergence of the **Escherichia coli** DnaK (Hsp70) and GroEL (Hsp60) chaperone machines. *Genetics* **174,** 1699–1707
19. Zylicz, M., Ang, D., Liberek, K., and Georgopoulos, C. (1989) Initiation of λDNA replication with purified host- and bacteriophage-encoded proteins. The role of the dnaK, dnaJ, and grpE heat shock proteins. *EMBO J.* **8,** 1601–1608
20. Zylicz, M. (1993) The *Escherichia coli* chaperones involved in DNA replication. *Philos. Trans. R. Soc. Lond. B Biol. Sci.* **339,** 271–278
21. de Crouy-Chanel, A., Kohiyama, M., and Richarme, G. (1995) A novel function of *Escherichia coli* chaperone DnaJ. Protein-disulfide isomerase. *J. Biol. Chem.* **270,** 22669–22672
22. Rüdiger, S., Schneider-Mergener, J., and Bukau, B. (2001) Its substrate specificity characterizes the DnaJ co-chaperone as a scanning factor for the DnaK chaperone. *EMBO J.* **20,** 1042–1050
23. Shimizu, T., Yoshii, A., Sakurai, K., Hamada, K., Yamaji, Y., Suzuki, M., Namba, S., and Hibi, T. (2009) Identification of a novel tobacco DnaJ-like protein that interacts with the movement protein of tobacco mosaic virus. *Arch. Virol.* **154,** 959–967
24. Champ, S., Puvirajesinghe, T. M., Perrody, E., Menouni, R., Genevaux, P., and Ansaldi, M. (2011) Chaperone-assisted excisive recombination, a solitary role for DnaJ (Hsp40) chaperone in lysogeny escape. *J. Biol. Chem.* **286,** 38876–38885
25. Cajo, G. C., Horne, B. E., Kelley, W. L., Schwager, F., Georgopoulos, C., and Genevaux, P. (2006) The role of the DIF motif of the DnaJ (Hsp40) co-chaperone in the regulation of the DnaK (Hsp70) chaperone cycle. *J. Biol. Chem.* **281,** 12436–12444
26. Erales, J., Lignon, S., and Gontero, B. (2009) CP12 from *Chlamydomonas reinhardtii*, a permanent specific "chaperone-like" protein of glyceraldehyde-3-phosphate dehydrogenase. *J. Biol. Chem.* **284,** 12735–12744
27. Grzesiek, S., Bax, A., Clore, G. M., Gronenborn, A. M., Hu, J. S., Kaufman, J., Palmer, I., Stahl, S. J., and Wingfield, P. T. (1996) The solution structure of HIV-1 Nef reveals an unexpected fold and permits delineation of the binding surface for the SH3 domain of Hck tyrosine protein kinase. *Nat. Struct. Biol.* **3,** 340–345
28. Ansaldi, M., Lepelletier, M., and Méjean, V. (1996) Site-specific mutagenesis by using an accurate recombinant polymerase chain reaction method. *Anal. Biochem.* **234,** 110–111
29. Panis, G., Duverger, Y., Champ, S., and Ansaldi, M. (2010) Protein-binding sites involved in the assembly of the KplE1 prophage intasome. *Virology* **404,** 41–50
30. Rodriguez, F., Arsène-Ploetze, F., Rist, W., Rüdiger, S., Schneider-Mergener, J., Mayer, M. P., and Bukau, B. (2008) Molecular basis for regulation of the heat shock transcription factor σ32 by the DnaK and DnaJ chaperones. *Mol. Cell* **32,** 347–358

DnaJ (Hsp40 Protein) Binding to Folded Substrate Impacts KplE1 Prophage Excision Efficiency

Tania M. Puvirajesinghe, Latifa Elantak, Sabrina Lignon, Nathalie Franche, Marianne Ilbert and Mireille Ansaldi

J. Biol. Chem. 2012, 287:14169-14177.
doi: 10.1074/jbc.M111.331462 originally published online February 28, 2012
